

Influence of Amorphous Nanodispersive SiO₂ Additive on Structure Formation and Properties of Autoclaved Aerated Concrete

Antanas LAUKAITIS^{1,2*}, Jadvyga KERIENĖ³, Modestas KLIGYS¹,
Donatas MIKULSKIS¹, Lina LEKŪNAITĖ¹

¹ Scientific Institute of Thermal Insulation, Vilnius Gediminas Technical University,
Linkmenų 28, LT-08217 Vilnius, Lithuania

² Department of Building Materials, Vilnius Gediminas Technical University,
Saulėtekio al. 11, LT-10223 Vilnius, Lithuania

³ Department of Chemistry and Bioengineering, Vilnius Gediminas Technical University,
Saulėtekio al. 11, LT-10223 Vilnius, Lithuania

Received 01 October 2009; accepted 01 July 2010

The influence of surfactant concentration and pozzolanic amorphous nanodispersive SiO₂ (ANS) additive on formation of autoclaved aerated concrete (AAC) structures and properties was investigated. It was established that in the AAC forming mixture the replacement of 1.0 % milled sand by ANS accounts for considerably higher crystallinity of hardened binding material, and that the plate-like shape of crystals generated in this case is typical to hydrosilicates with lower ratio C/S. The formation of such AAC structure conditioned increase in compressive strength by 20.0 %, bending strength by 31.0 and decrease in shrinkage at temperature of 700 °C by 0.1 % versus AAC without surfactant and ANS. Basing on the results of investigations, a hypothesis was framed to say that ANS added to AAC forming mass serve as nucleators during the hardening of concrete, stimulating higher crystallinity in the hardened structure of binding material than that without this additives and improving AAC mechanical properties. In addition to this impact, the ANS additive helps to form the crystalline structure, in this way evidencing existence of compounds with lower ratio C/S in AAC hardening structure, as well as to increase thermal resistance of concrete.

Keywords: aerated autoclaved concrete, amorphous nanodispersive SiO₂, structure formation, mechanical strength.

INTRODUCTION

At the beginning of hardening process of aerated autoclaved concretes (AAC), as well as of cement-based concretes (CC), the formation of amorphous nanostructure takes place. Of course, it is understandable that in case of AAC hardening, the formation of amorphous nanostructure, accompanied by crystallization and growth of crystals are going on at a higher rate than in case of CC hardening.

The researches on formation of amorphous nanostructure during CC hardening and impact of various technological factors on this process, as well as impact of nanostructure, which forms at the beginning of hardening, on properties of hardened CC started as early as before more than fifty years. The work [1] cites the study of T. C. Powers and T. L. Brownyard published in 1948 where it is said about the paste mixed out of cement and water as having properties similar to colloids and gels – colloid coagulation products. The authors of this work indicate that during the intervening half-century of research, the colloidal properties of the C-S-H gel have often been downplayed in favour of structural interpretation based on naturally occurring minerals such as tobermorite and jennite. Because these minerals have a layered structure, the existence of “interlayer spaces” in the C-S-H gel containing strongly adsorbed water was postulated. Ten years ago in the work [2], basing on the results of investigations performed by using of modern methods, such model was proposed for the structure of aggregates of

roughly equiaxed colloidal-scale particles with no long-range layered structure on a scale greater than a few nanometers. According to the model the smallest unit C-S-H is a small tobermorite-like or jennite-like particle.

These smallest fundamental units are packed together irregularly into structures called globules and globules are packed together to form light density (LD) and high density (HD) structures [2]. The spaces between the smallest units are analogous to the interlayer space in layer-based models. The spaces between the globules are the gel porosity that is intrinsic to C-S-H. The spaces between the LD and HD particles are large gel pores that might be considered small capillary pores.

It is noted [1] that along with increase in temperature, the speed of condensation for C-S-H gel aggregates forming particles is increasing, as well as C-S-H density, meanwhile the irreversible shrinkage and creep of concrete decrease. In the works [3, 4] it is shown that the pozzolanic amorphous nanodispersive SiO₂ additive (ANS) exerts a great influence on process of cement hardening and preconditions the formation of CC hardening structure much denser than that without this additive, as well as the improvement of properties of concrete.

The above discussed literature data show that a relation exists between nanostructure of cement-based materials and their properties and, that qualitatively new cement-based materials can be obtained by employing nanotechnologies and that one of such technologies is application of ANS.

At the beginning of hardening process of AAC, like cement-based concretes, the formation of hydrosilicates of amorphous state and nanostructures is taking place.

*Corresponding author. Tel.: +370-5-2750001; fax: +370-5-2750001.
E-mail address: antanas.laukaitis@termo.vgtu.lt (A. Laukaitis)

Therefore, one can expect that the properties of these concretes can be altered by employing nanotechnologies, and namely one of them: application of pozzolanic ANS. We failed to find in literature any researches, which dealt with application of this additive for modification of AAC.

On the other hand, since in AAC the transit of amorphous structure into crystalline one and growth of crystals go on very rapidly in comparison with CC, the formation of crystalline structure can be acted on by introduction of additives, which nucleate centers of crystallization. It is known that nano-size particles can serve as centers of crystallization, nucleators, and that on surface of these nano-size particles the nuclei of crystals may appear.

Basing on the considerations set forth above, we formulated the following purpose of this work: to estimate the impact of pozzolanic ANS additive on structure formation and properties of AAC.

MATERIALS AND EXPERIMENTAL

The forming mixtures of AAC were prepared using the raw materials described below. Milled lime (CL90 according to EN 459-2:2001 requirements), activity 91.6 %, slaking period 5 min., slaking temperature 55 °C, produced by Lithuanian company “NAUJASIS KALCITAS”. The quartz sand (according to EN 196-6:1996 requirements), produced by Lithuanian company “ANYKŠČIŲ KVARCAS”. The chemical composition of milled lime and sand is presented in Table 1.

The quartz sand was milled to fineness of 2766 cm²/g and 4750 cm²/g. The distribution of particles by size in sand samples of specified fineness is provided in Fig. 1. Quartz sand with fineness of 2766 cm²/g was used in production of all AAC sample series investigated in this work, except for samples used for investigation of impact of milled sand fineness on formation of AAC structure.

As a gas-generating agent, in AAC forming mixtures, aluminium paste “ALBO SCHLENK DEG 4508/70” was used. The specific surface is 18000 cm²/g, and content of pure aluminium in the paste – 70 %.

In the work 0.5 %, 1.0 % and 1.5 % of milled quartz sand was replaced by ANS (“SILIMIC”). ANS chemical composition is presented in Table 1, the shape and sizes of ANS particles showed in Fig. 2. The photo of ANS showed that this material is very finely dispersed. The size of its finest particles is in the range from 20 nm to 80 nm. The amount of the finest particles is from 30 % to 40 % of the overall volume of this material. The size of the biggest particles is from 300 nm to 400 nm.

For enough distribution of abovementioned ANS in AAC forming mixtures, the surfactant “UFAPORE TCO” was used in amount of 0.003 % (of solids dry mass). The influence of mentioned surfactant in higher concentration (0.010 % of solids dry mass) on the properties of AAC samples was also established.

The compositions of AAC forming mixtures were selected basing on methodical requirements [5]. The activity of mixtures expressed in content of active CaO and MgO, the only binding material being lime, was 20.0 %. Water-solids ratio – 0.54 content of aluminium paste – 0.18 % (of solids dry mass), binder-sand ratio – 1 : 2. The

compositions of AAC forming mixtures are presented in Table 2.

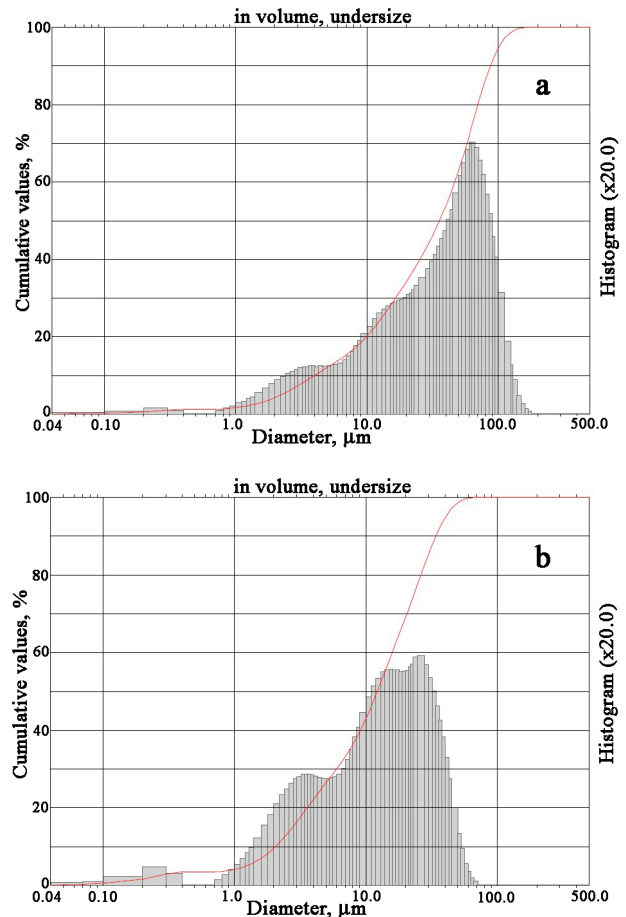


Fig. 1. Distribution of particles by size in milled sand samples of fineness of 2766 cm²/g (a) and 4750 cm²/g (b)

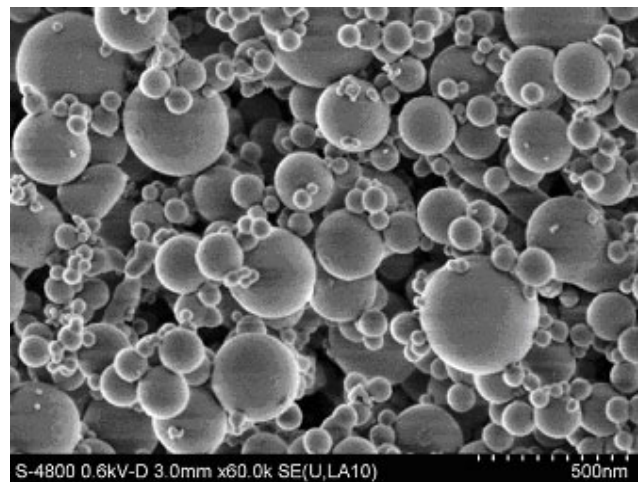


Fig. 2. Morphology of ANS additive (magnification – ×60 000). The detailed description provided in the text

The distribution of quartz sand particles in each individual sample of milled sand was determined by laser analyzer “FRITCH ANALYSETE 22”.

The components of forming mixtures were mixed in the vessel of 2 liters using the hand mixer “KENWOOD” kMix HM 790 (maximal power 400 W, rotation N5). The sequence of component loading and duration of mixing is presented in Table 3.

Table 1. Chemical composition of raw materials and additives

Raw materials and additives	Composition (in mass %)										Other, %
	SiO ₂	Al ₂ O ₃	Fe ₂ O ₃	CaO	MgO	K ₂ O	Na ₂ O	SO ₃	R ₂ O	C	
Lime	4.05	2.21	0.88	89.24	2.38	–	–	–	0.37	–	0.87
Sand	97.89	0.60	0.46	0.72	–	–	–	0.06	0.10	–	0.17
ANS	88.00	–	1.50	1.00	1.50	2.00	0.60	–	–	1.50	3.90

Table 2. Forming mixture components mass (in grams) and volume of water (in milliliters)

Components	Forming mixture (activity 20.0%)					
	Sample 1	Sample 2	Sample 3	Sample 4	Sample 5	Sample 6
	Without surfactant and ANS	With surfactant and without ANS		With surfactant (0.003%) and ANS		
		0.003 %	0.010 %	0.50 %	1.00 %	1.50 %
Lime	137.00	137.00	137.00	137.00	137.00	137.00
Sand	412.00	411.98	411.95	409.92	407.86	405.80
Aluminium paste	1.1000	1.1000	1.1000	1.1000	1.1000	1.1000
ANS	–	–	–	2.0600	4.1200	6.1800
Surfactant	–	0.0165	0.0550	0.0165	0.0165	0.0165
Water	300.00	300.00	300.00	300.00	300.00	300.00

Table 3. Sequence of component dispensing and duration of mixing for production of forming mixtures

Components	Duration of mixing, min
1. Water + sand	3.0
2. Water + sand + ANS (mixed with surfactant)	5.0
3. Water + sand + ANS (mixed with surfactant) + lime	1.0
4. Water + sand + ANS (mixed with surfactant) + lime + aluminium paste	1.0
Overall: 10.0	

After adding water to forming mixture with ANS, for even distribution of additive, the mixture was dispersed by ultrasonic disperser “UZDN-2T” (frequency 22 kHz, power 480 W).

The prepared AAC forming mixtures were poured into molds of (70×70×70) mm for compressive and (40×40×160) mm for bending strengths. The expanded forming mixture was kept in molds for 3.0 h, then, after cutting off the heap of forming mixture, the molded samples were hardened in the laboratory autoclave of 100 liters capacity, following the specified mode of hardening (5+10+5) h, at water vapor temperature of 176 °C what corresponds to pressure of 0.8 MPa. After hardening, the samples were dried to constant mass in the conditioning oven at temperature of 105 °C ±5 °C.

The compressive and bending strengths of AAC samples were determined according to the requirements of EN 679:2000 and EN 1351:1996. The press “TINIUS OLSEN H200KU” was used. The loading rate of samples during compression was 60.0 N/s, and bending – 14 N/s. 3 samples of each batch were subjected to testing. As actual densities of samples from various batches varied, the obtained actual compressive and bending strength values were recalculated according to the technique [5] for selected density 450 kg/m³.

The X-ray analysis was performed by diffractometer “DRON-7”. Anode – Cu, filter – Ni, anode voltage – 30.0 kV, anode current – 8 mA, goniometer apertures (0.5; 1.0;

1.5) mm. The phase composition was determined employing ICDD database.

Differential scanning calorimetry (DSC) was employed for measuring phase transformation of the AAC samples of 50 mg weight, at a heating rate of 10 °C/min, the temperature ranged from 25 °C to 1000 °C under air atmosphere. The tests were carried out on a “LINSEIS STA PT-1600” instrument.

Thermal analysis was performed by the dilatometer “LINSEIS L76”. Temperature rise speed to 700 °C was 5.0 °C/min, exposure time of AAC samples in 700 °C temperature was 300 min. Diameter and length of AAC samples 5.0 mm and 50.0 mm accordingly.

The microstructure was investigated by scanning electron microscopes (SEM). The morphology of ANS particles was investigated by SEM S-4800 of the firm “HITACHI” (without coating by conductive layer, accelerating voltage 0.6 kV), the microstructure of AAC samples was investigated by SEM JSM 6490 LV of the firm “JEOL” (coated in vacuum by conductive carbon layer, accelerating voltage 20.0 kV).

RESULTS AND DISCUSSION

The average values of compressive strength of AAC samples are shown in Fig. 3. The average value of compressive strength of AAC samples without surfactant and ANS (Fig. 3, column a) was 3.00 MPa. It was fixed that very small amount (0.003 %) of surfactant (Fig. 3,

column b) slightly increased (3.3 %) the compressive strength of AAC samples. The average value of compressive strength decreased about 7.1 % (Fig. 3, column c), when surfactant in higher concentration (0.010 %) was used. Resuming obtained results we can maintain that low concentrations of surfactant have no influence on the compressive strength of AAC samples.

When 1.0 % of milled sand was replaced by ANS and surfactant concentration is 0.003 %, the highest average value of compressive strength (3.60 MPa) of AAC samples was obtained (Fig. 3, column e). That means that mentioned replacements result in increase of compressive strength of AAC samples by 20.0 % versus samples without these additives.

In case of replacement of milled sand (0.5 % or 1.5 %) by ANS and at surfactant concentration of 0.003 %, the change in compressive strength of AAC samples was not remarkable versus samples without ANS (Fig. 3, columns d and f). For lightweight AAC the most optimal replacement of milled sand by ANS is 1.0 % as higher amounts of it can not be dispersed well in the AAC forming mixture.

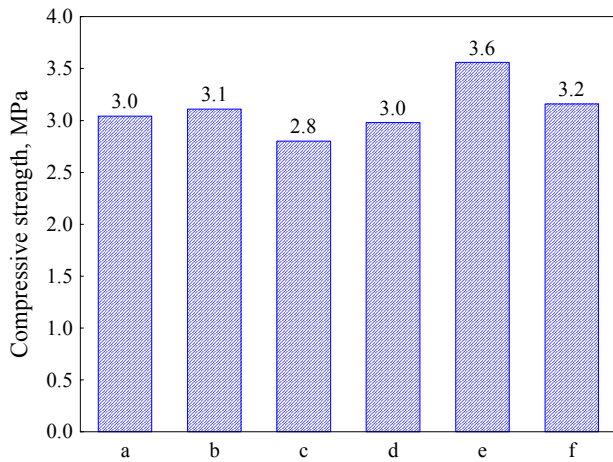


Fig. 3. The compressive strength of AAC samples: a – sample 1; b – sample 2; c – sample 3; d – sample 4; e – sample 5; f – sample 6

The average values of bending strength of hardened AAC samples are shown in Fig. 4. The average value of bending strength of AAC samples without surfactant and ANS (Fig. 4, column a) was 1.30 MPa. Obtained results confirmed compressive strength results, that surfactant in lower concentration such as 0.003 %, has no influence on bending strength (1.30 MPa) of AAC samples (Fig. 4, column b). On the other hand, higher concentration (0.010 %) of surfactant 30 % decreased bending strength of AAC samples (Fig. 4, column c).

When 1.0 % of milled sand was replaced by ANS and surfactant concentration is 0.003 %, the highest average value of bending strength (1.70 MPa) of AAC samples was also obtained (Fig. 4, column e). These bending strength results confirmed compressive strength results that mentioned replacements result in increase of bending strength of AAC samples by 31.0 % versus samples without these additives.

In case of replacement of milled sand (0.5 % or 1.5 %) by ANS and at surfactant concentration of 0.003 %, the

change in bending strength of AAC samples was also not remarkable versus samples without ANS (Fig. 4, columns d and f). It confirmed results of compressive strength which have been described above.

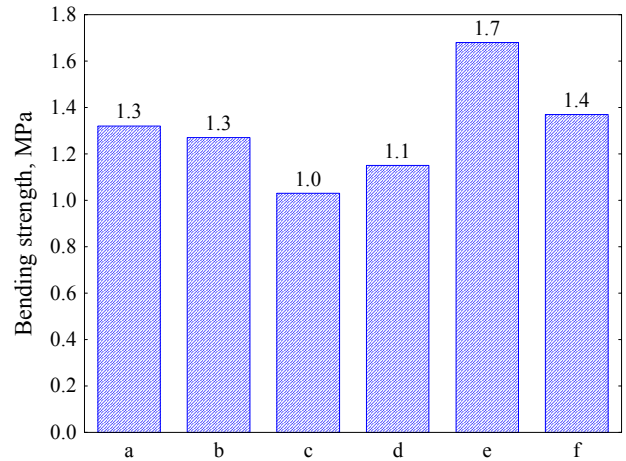


Fig. 4. The bending strength of AAC samples: a – sample 1; b – sample 2; c – sample 3; d – sample 4; e – sample 5; f – sample 6

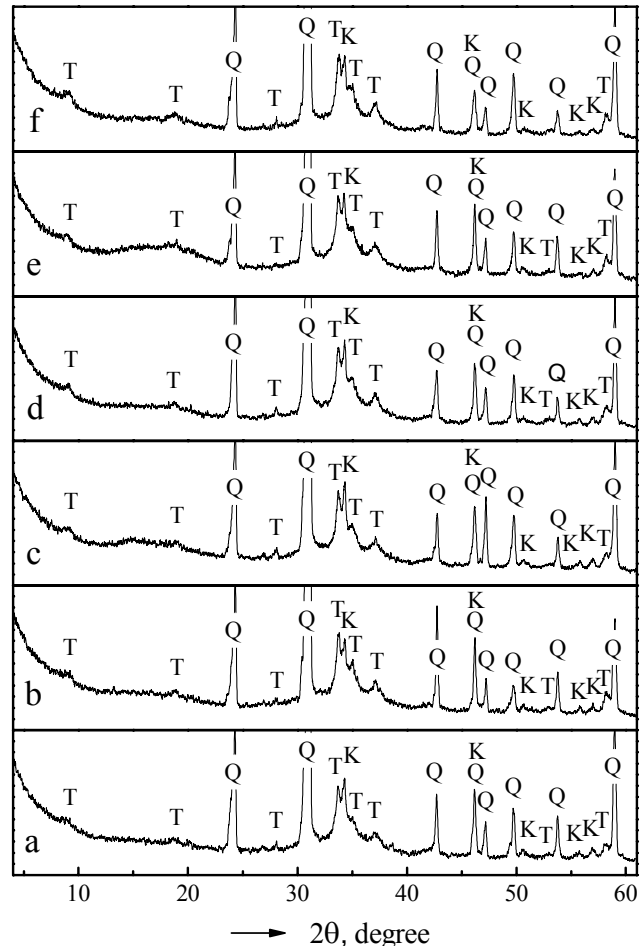


Fig. 5. XRD patterns of AAC samples: a – sample 1; b – sample 2; c – sample 3; d – sample 4; e – sample 5; f – sample 6. Q – quartz; T – tobermorite; K – calcite

By XRD investigations it was established (Fig. 5) that during hardening in both AAC samples without surfactant and ANS (Fig. 5, a) and samples where 0.5, 1.0 or 1.5 % of milled sand is replaced by ANS and surfactant in

concentration 0.003 % (Fig. 5, d, e and f) tobermorite formed and some non reacted sand remained (as seen from the X-ray peaks corresponding to quartz).

It was established that the intensity of tobermorite-corresponding peaks in the samples, where 0.5 %, 1.0 % or 1.5 % of milled sand is replaced by ANS, is higher than that of samples without ANS. The intensity of quartz-corresponding peaks in the mentioned samples is also higher than that of samples without ANS. This is quite understandable, since $\text{Ca}(\text{OH})_2$ reacts easier with amorphous SiO_2 than with sand-composing crystalline SiO_2 . In the presence of both amorphous and crystalline SiO_2 in the system, the reaction runs, the first thing, with amorphous SiO_2 . The XRD patterns show that hardened samples contain a small quantity of calcite.

The results of DSC analysis (Fig. 6) confirmed the XRD analysis results. The DTA curves of all samples – without surfactant and ANS (Fig. 6, a) and with surfactant and ANS (Fig. 6, b–f) – have effects corresponding to tobermorite (egzo-effect at $819 \div 821$ °C), quartz (endo-effect at 568 °C or 569 °C) and calcite (endo-effect at 723 °C, 724 °C or 729 °C). Furthermore, basing on the results of DSC analysis (Fig. 6, a–f), one can maintain that all AAC samples have the amorphous CSH phase (endo-effect within temperatures of $100 \div 250$ °C).

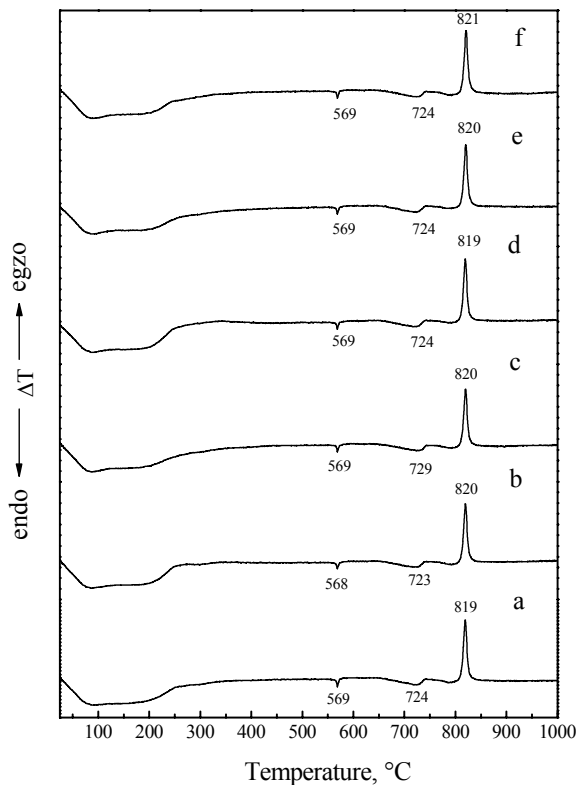


Fig. 6. The DTA curves of AAC samples: a – sample 1; b – sample 2; c – sample 3; d – sample 4; e – sample 5; f – sample 6

The thermal analysis (Fig. 7) showed that the change in length of AAC samples without surfactant and ANS additives at temperature of 700 °C made 1.33 %. The formation of binding material of greater crystallinity in AAC samples with low concentrations of surfactant, and different amounts of ANS additives conditioned higher thermal resistance. After replacing of 0.5 %, 1.0 % and

1.5 % milled sand by ANS additive, the change in length of AAC samples was in that order: 1.29 %, 1.24 % and 1.28 %. The AAC samples with low concentration (0.003 %) of surfactant and without ANS additive showed enough low value (1.19 %) of change in length. On the other hand increased to 0.010 % concentration of surfactant determines noticeably higher change in length (1.48 %). This factor indicates that more attention should be set to the applience of surfactants even if they used in very low concentrations.

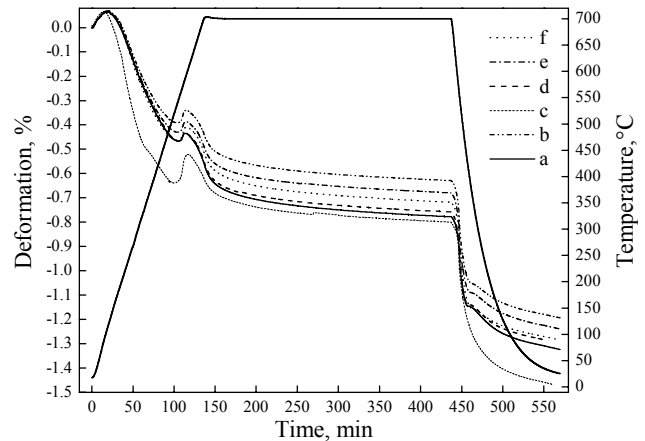


Fig. 7. The dilatometric curves of AAC samples: a – sample 1; b – sample 2; c – sample 3; d – sample 4; e – sample 5; f – sample 6

The differences in microstructure of hardened AAC samples are most easily observable at investigating of microstructure in surface layer of pore walls where are more favoring conditions for formation and free growth of hydrosilicate crystals than in any other place of hardening AAC volume because of accumulation of water vapor in pores during hardening. Furthermore, at breaking of sample for investigation of its structure, the pore walls remain undestroyed and their crystalline structure is not injured. Therefore, for comparison of binder microstructure, which formed during hardening, the investigations of pore wall microstructure were performed in the samples.

The results of investigations of microstructure (Fig. 8) show that the ANS additive has a very strong impact on formation of AAC microstructure during AAC hardening. In the sample without ANS additive on surface layer of pore walls (Fig. 8, a and b) much amorphous phase is accumulated and crystals, generated together with it, are mostly needle-like. Meanwhile on surface layer of pore walls in AAC with ANS (Fig. 8, d and e) no amorphous phase is observable; here we can see crystals shaped as plate-like strips. So, the crystallinity of this sample is considerably higher than that of AAC without ANS and the shape of crystals is also different.

In the partitions dividing the pores, both in case of AAC without ANS and with ANS, the particles of milled sand are found. In the sample without ANS they contact worse with binding material than in the sample with this additive (please compare Fig. 8, c with Fig. 8, f).

The described differences of microstructure are predetermined by activity of ANS higher than that of milled sand what conditions a higher speed of the reaction between alkaline $\text{Ca}(\text{OH})_2$ and acidic (SiO_2) components and formation of hydrosilicates with lower ratio C/S.

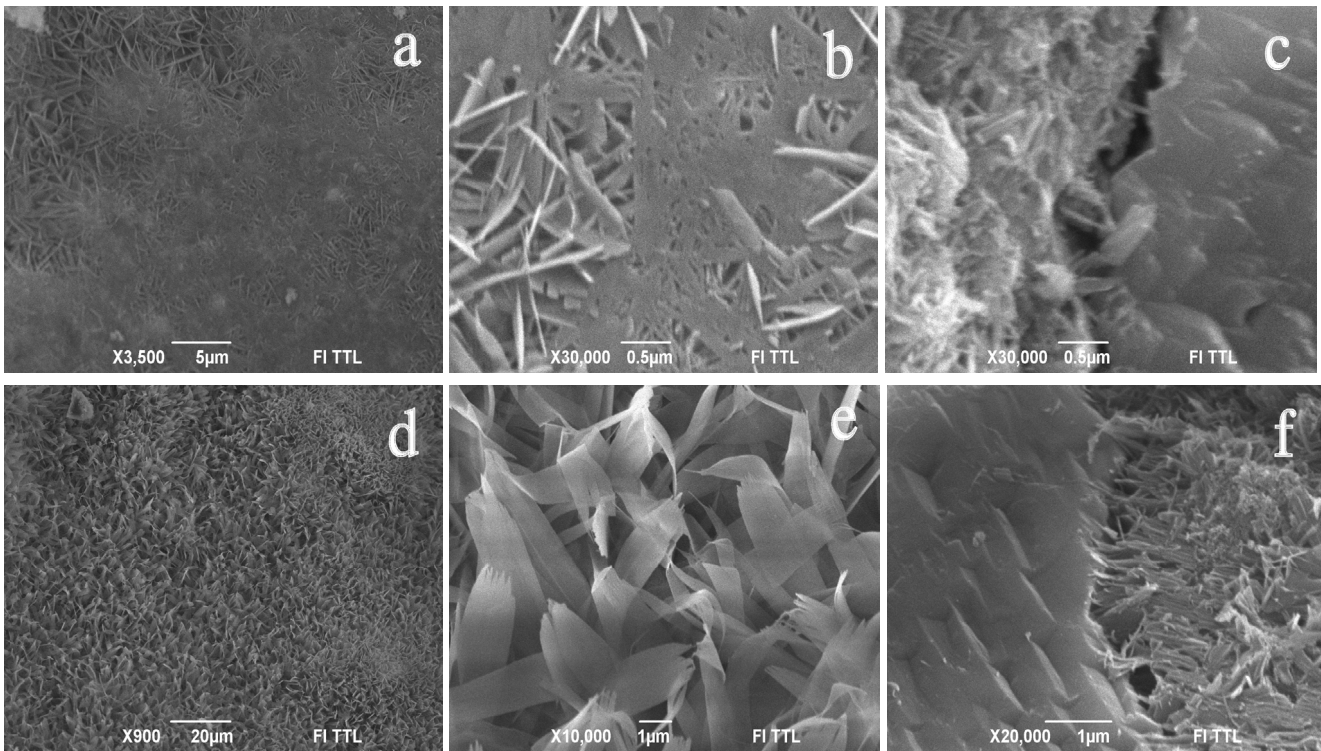


Fig. 8. Fragments of fracture surface microstructure of AAC samples: a, b, c – without surfactant and ANS additive (sample 1); d, e, f – with surfactant (0.003 %) and 1.0 % sand replaced by ANS (sample 5); a, b, d, e – microstructure of pore wall; c, f – contact zone of sand particle – binding material (in the photo “c” the sand particle is on the right, in the photo “f” the sand particle is on the left)

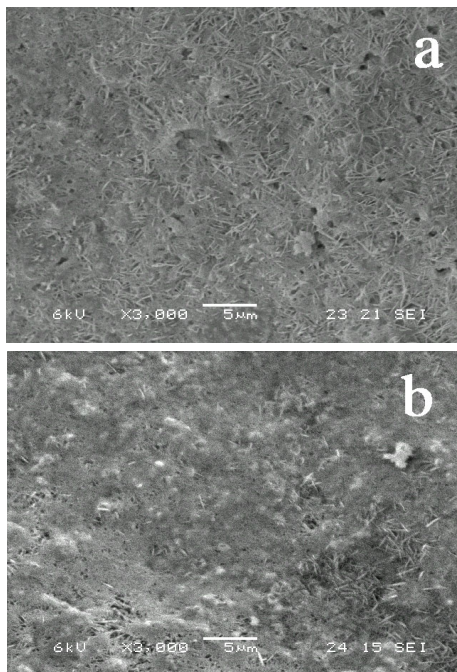


Fig. 9. Fragments of microstructure of AAC pore wall: a – fineness of milled sand 2766 cm²/g, b – fineness of milled sand 4750 cm²/g. Magnification ×3 000

We established that instead of additive ANS using sand milled finer by 1.7 times, i.e. 4750 cm²/g instead of 2766 cm²/g in AAC production, the compressive strength increased by 7.0 %. SEM investigations showed (Fig. 9) that in this case in the binding material a greater quantity of amorphous phase is generated than using sand with fineness of 2766 cm²/g.

We suppose that the reason of this phenomenon lies in activity of sand, which increases after finer milling (up to 4750 cm²/g) because of increased surface defectiveness of particles. Along with increase in activity of sand, the speed of its reaction with water vapor in alkaline environment increases. The reaction also accelerates due to increased surface area of sand particles after finer milling of sand.

Thank to all this, during the reaction of sand with water vapor, more of gel silicate phase is forming than in case of sand with fineness of 2766 cm²/g. Upon comparison of the results of investigation of this microstructure with the results obtained after replacement of 1.0 % milled sand by ANS during mixing of AAC samples, we can frame the following hypothesis. In the AAC hardening process the nano-size particles of ANS serve not only as a SiO₂ source for formation of gel-state hydrosilicates, but also as nucleators of crystallization centers for hydrosilicates. Similarly, the particles of alite serve as centers of nucleation, which is the main phase of cement, as indicated in the review of researches provided in the work [6] in which the modeling of nucleation and crystal growth during the hydration of alite by a new method of modeling [7] was performed. The main motive for framing this hypothesis is that after fine milling of sand, thank to increase in its activity and contact area of reacting materials, more gel phase emerges. However, in this case no centers of crystallization are introduced as in case of ANS, therefore, the crystallinity of hardened AAC mass remains lower than that of AAC with ANS.

So, the obtained data of this work show that in case of AAC similar as in the case of CC [8], the formation of nano- and microstructures of these materials account for their properties.

CONCLUSIONS

1. Replacement of 1.0 % milled sand by ANS, and usage of surfactant in low concentration in the AAC forming mixture, conditions considerably higher crystallinity of hardened binding material, and in this case the plate-like shape of born crystals is typical to hydrosilicates of lower ratio C/S. The formation of such AAC structure accounts for increase in compressive strength by 20.0 %, bending strength by 31.0 % and decrease in shrinkage at temperature of 700 °C by 0.1 % versus AAC without surfactant and ANS.
2. Basing on the results of investigations, a hypothesis is framed to say that the additive of AAC forming mixture, such as ANS, serve as nucleators during the hardening of this concrete and stimulate the formation of binder hardening structure with higher crystallinity than that without these additives, as well as the improvement of AAC mechanical properties.
3. The ANS additive also conditions the origination of compounds having hardening structure characteristic for the lower ratio C/S compounds and the increase in thermal resistance of AAC.

Acknowledgments

The research was supported by Lithuanian State Science and Studies Foundation (Project Nano-CSM).

REFERENCES

1. **Thomas, J. J., Jennings, H. M.** A Colloid Interpretation of Chemical Aging of the C-S-H Gel and its Effects on the Properties of Cement Paste *Cement and Concrete Research* 36 2006: pp. 31–38.
2. **Jennings, H. M.** A Model for the Microstructure of Calcium Silicate Hydrate in the Cement Paste *Cement and Concrete Research* 30 2000: pp. 101–116.
3. **Jo, B. W., Kim, Ch. H., Tae, Ghi Ho, Park, J. B.** Characteristics of Cement Mortar With Nano-SiO₂ Particles *Construction and Building Materials* 21 2007: pp. 1351–1355.
4. **Kropa, A., Kowald, T., Trettin, R.** Hydration Behavior, Structure and Morphology of Hydration Phases in Advanced Cement-based Systems Containing Micro and Nanoscale Pozzolan Additives *Cement and Concrete Research* 38 2008: pp. 995–962.
5. **Laukaitis, A.** Composition Calculations and Properties Investigation Methods of Porous Concrete. Vilnius: Thermal Insulation, 1996: 14 p. (in Lithuanian).
6. **Bichnoi, S., Scrinever, K. L.** Studying Nucleation and Growth Kinetics of Alite Hydration Using μic *Cement and Concrete Research* (article in press) 12 pages.
7. **Bichnoi, S., Scrinever, K. L.** μic : A New Platform for Modeling the Hydration of Cements *Cement and Concrete Research* 39 2009: pp. 255–265.
8. **Monteiro, P. M. J., Kirchheim, A. P., Chae, S., Fisher, P., MacDowell, A. A., Schaible, E., Wenk, H. R.** Characterizing the Nano and Microstructure of Concrete to Improve Its Durability *Cement and Concrete Composites* 31 2009: pp. 577–584.

Presented at the National Conference "Materials Engineering'2009" (Kaunas, Lithuania, November 20, 2009)

DOI: 10.5755/j02.ms.26078